Effect of configurational order on the magnetic characteristics of Co-Ni-Ga ferromagnetic shape memory alloys

Navdeep Singh,[1] Ebubekir Dogan,[1] Ibrahim Karaman,[1,2] and Raymundo Arróyave[1,2]
[1]*Department of Mechanical Engineering, Texas A&M University, College Station, Texas 77843, USA*
[2]*Materials Science and Engineering Program, Texas A&M University, College Station, Texas 77843, USA*
(Received 29 June 2011; revised manuscript received 29 August 2011; published 1 November 2011)

In most of the ternary (and higher-order) ferromagnetic shape memory alloys (FSMAs) with compositions close to the A_2BC stoichiometry, the austenite phase exhibits $L2_1$-type ordering. Recent investigations of the Co-Ni-Ga FSMA system, however, suggest that the austenite phase has $B2$-type ordering, although definite confirmation remains elusive. In this work, we present a theoretical investigation of the effect of configurational order on the magnetic properties of the ordered ($L2_1$) and disordered ($B2$) FSMA Co_2NiGa. Through the use of calculations based on density functional theory, we predict the structural and magnetic properties (including magnetic exchange constants) of ordered and disordered Co_2NiGa alloys. We validate our calculation of the magnetic exchange constants by extracting the Curie temperatures of the austenite and martensite structures and comparing them to experimental results. By constructing a q-state Potts magnetic Hamiltonian and through the use of lattice Monte Carlo simulation, we predict the finite-temperature behavior of the magnetization and magnetic susceptibility as well as the magnetic specific heat and entropy. The role of configurational order in the magnetic properties of the phases involved in the martensitic phase transformation is discussed, and predictions of the magnitude of the magnetic contributions to the transformation entropy are presented. The calculations are compared to experimental information available in the literature as well as experiments performed by the authors. It is concluded that in FSMAs magnetism plays a fundamental role in determining the relative stability of the austenite and martensite phases, which in turn determines the martensitic transformation temperature M_s, irrespective of whether magnetic fields are used to drive the transformation.

DOI: 10.1103/PhysRevB.84.184201 PACS number(s): 75.25.−j, 75.40.Mg

I. INTRODUCTION

In recent years, research on ferromagnetic shape memory alloys (FSMAs) has gained significant momentum owing to their remarkable multifunctional behavior, not only related to the shape memory effect, giant magnetostriction, and coupled magnetomechanical phase transformations but also—at least in some systems—due to other magnetic phenomena such as the giant magnetocaloric effect and magnetoresistance.[1,2] Ni-Mn-Ga-based FSMAs have been studied in great detail since the first reported large magnetic-field-induced strains in these alloys.[3] Despite their remarkable magnetic-field-induced shape change levels, these materials suffer from relatively low Curie temperature (∼373 K), intrinsic brittleness, relatively low martensitic transformation temperatures, and low actuation stress levels.[4,5] In order to increase the martensitic start transformation temperature (M_s), Ga is replaced with Mn, but the resulting alloys have poor magnetic properties due to antiferromagnetic interaction between the Mn atoms occupying the original Mn lattice sites and those occupying Ga lattice sites.[6,7] Some of these problems have been solved by substituting Mn with Co.

Co_2NiGa alloys have been proposed as a possible alternative to Ni-Mn-Ga alloys due to their higher transformation and Curie temperatures as well as better ductility.[8] In most ternary and higher-order FSMAs the austenite phase that undergoes the martensitic transformation has an $L2_1$-type ordered structure with the A_2BC stoichiometry. This structure can actually be visualized as two interpenetrating bcc lattices with $B2$-type ordering, in which the majority atom (A) occupies the body-centered sites and the minority atoms (B and C) occupy alternate corners. In contrast to what is observed in most Heusler-type FSMAs, the austenite phase in Co-Ni-Ga alloys has a stoichiometry close to Co_2NiGa but seems to have $B2$-type ordering (β phase) as opposed to $L2_1$, although there is no definite conclusion in this regard.[9,10]

Judicious manipulation of the composition and heat treatment temperature in Co-Ni-Ga SMAs can introduce order in disordered systems as well as resulting in a multiphase microstructure composed of the transformable β phase, accompanied by a much more ductile fcc-type (γ) phase as well as intermetallic precipitates (γ') based on the $L1_2$ structure. The γ phase greatly enhances the high-temperature workability and room-temperature ductility of these alloys but can also strongly affect the shape memory properties and martensitic transformation temperatures resulting in a wide range of operating temperatures.[10–13]

Atomic ordering has been known to influence the transformation behavior of SMAs. The order-disorder transition, long-range ordering, and effect of ordering on the phase transformation temperatures in various shape memory alloys have been studied experimentally and numerically.[14–21] The effect of atomic ordering on the transformation temperatures has been experimentally investigated in $Ni_{45}Co_5Mn_{36.7}In_{13.3}$ (Ref. 19) and $Ni_{55}Fe_{20}Al_{25}$ (Ref. 21) FSMAs. In the case of $Ni_{45}Co_5Mn_{36.7}In_{13.3}$, fully ordered $L2_1$and partially ordered $B2$ phases have been obtained by annealing the samples at 623 and 923 K, while for $Ni_{55}Fe_{20}Al_{25}$ an ordered phase has been obtained by annealing at 793 K and the site-disordered phase by simply quenching the samples from higher temperatures. For the ordered systems, the Curie temperature in the austenite phase and magnetization levels in the martensite phase are higher but the martensite transformation temperature is lower than in the partially ordered or disordered phase. The

 ©2011 American Physical Society

decrease in the martensitic transformation temperatures with ordering of the austenite phase to $L2_1$ has also been reported previously in NiMnAl FSMAs.[20] In the case of $Ni_{55}Fe_{20}Al_{25}$, austenite and martensite phases coexist in the ordered phase for a wide temperature range, while for the disordered phase the martensitic transformation is well defined.[21]

Ordered and disordered alloys of Co_2NiGa have also been studied experimentally.[9] Comparison of the magnetic properties of ordered and disordered phases suggest that ordering can increase the magnetization by 40%. This result is in contrast to those reported for $Ni_{55}Fe_{20}Al_{25}$, in which the specific magnetization of the ordered phase is lower than that of the disordered phase.[21] The decrease in magnetization of the disordered phase in Co_2NiGa is attributed to the sharp decrease in the magnetic moment of the Co atoms surrounded by a large number of Co or Ni atoms in the disordered alloys.[9]

In previous work by the one of the authors,[22] *ab initio* calculations have been performed to study the phase stability, phase transformation, and electronic properties of the stoichiometric ordered and disordered Co_2NiGa alloys. The ordered structure was modeled as $L2_1$ while the disordered phases were modeled with a $B2$-type structure. Austenite has been found to be less stable than martensite in both the ordered and disordered states.[22] Specifically, Bain-path studies showed that the austenite phase is metastable (at best) with respect to volume-conserving tetragonal distortions. It was suggested that the relative instability of austenite can be attributed to the decrease in magnetism due to increase in magnetic disorder and to the increase in the volume of the system due to the lattice thermal expansion as the temperature increases.[22] On the other hand, for the Ni-Mn-Ga alloys, the stability of the tetragonal (martensite) vs the cubic (austenite) structure is associated with the Jahn-Teller distortion.[23] From electronic structure calculations, instability in Ni_2MnGa is due to the lack of hybridization between $3d$ spin-down Mn and Ni states, while in Co_2NiGa, the instability is due to the location of the Fermi level at the beginning of low-lying spin-down antibonding states.[22] Similar theoretical work by Siewert *et al.*[24] on Co-Ni-Ga Heusler alloys seems to corroborate the results presented in Ref. 22, although in the former case the effect of disorder on the stability of the austenite phase was examined by exploring conventional Heusler $L2_1$ ordering as well as so-called inverse Heusler configurations in which one of the majority atoms—Co in this case—is replaced by either of the minority components—Ni or Ga in this instance.

The present work has been performed to elucidate the effect of atomic ordering on the magnetic properties of Co-Ni-Ga alloys using experiments, *ab initio* calculations, and Monte Carlo simulations. As described in previous work,[22] a body-centered structure with $B2$-type ordering has been used to mimic the disordered state of the system and an $L2_1$ structure has been used to mimic the fully ordered state. We consider the stoichiometric Co_2NiGa configuration as well as off-stoichiometric compositions that have been widely studied experimentally. In addition, we present results from the characterization of off-stoichiometric Co-Ni-Ga alloys prepared by the authors. For the simulation of the off-stoichiometric compositions, we consider different degrees of order by varying the atomic occupation of the different sublattices of the $L2_1$ structure as well as by considering the fully disordered $B2$ configuration. We examine the effects of configuration on magnetic properties by calculating the magnetic exchange constants, report the calculated saturation magnetization, Curie temperatures, and structural parameters for all the configurations considered in this work, and compare these results with available experimental information. For the stoichiometric compositions, we calculate the magnetization, magnetic susceptibility, magnetic specific heat, and magnetic entropy by means of Monte Carlo simulations assuming a q-state Potts Hamiltonian and using magnetic exchange parameters obtained from *ab initio* calculations.

II. SIMULATION METHODS

Electronic structure calculations are carried out using the spin-polarized relativistic Korringa-Kohn-Rostoker (SPRKKR) band structure code.[25,26] This code is based on the KKR–Green's function formalism that makes use of multiple-scattering theory, and the electronic structure is expressed in terms of the corresponding Green's function as opposed to Bloch wave functions and eigenvalues. In this code, configurational disorder is treated through the coherent potential approximation (CPA). The exchange-correlation potential was modeled within the generalized gradient approximation of Perdew, Burke, and Ernzerhof. The first step in these calculations is to determine the optimized lattice parameter for all the structures. These calculations were performed using a spin-polarized scalar-relativistic Hamiltonian with full potential using an orbital momentum cutoff $l_{\max} = 3$ on a grid of $22 \times 22 \times 22$ **k** points and 30 points on the complex energy path. All calculations converged to 0.13 meV of total energy. For the optimized lattice parameter, the self-consistent potential is calculated. This new self-consistent potential is then used to calculate the Heisenberg magnetic exchange coupling parameters J_m^{ij}, using the equation proposed by Liechtenstein *et al.*[27]

The magnetic exchange parameters can be used to calculate the Curie temperature of the system. For a multilattice system, the Curie temperature of the system using the mean-field approximation (MFA) can be obtained by solving the following coupled equations:[28,29]

$$\frac{3}{2}k_B T_c^{MFA} = \sum_{\nu} J_{m,0}^{\mu\nu}\langle e^{\nu}\rangle \tag{1}$$

and

$$J_{m,0}^{\mu\nu} = \sum_{R\neq 0 \text{ when } \mu=\nu} J_{m,0R}^{\mu\nu}. \tag{2}$$

In Eq. (2), the magnetic exchange parameter $J_{m,0}^{\mu\nu}$ is obtained by summing all exchange parameters involving the sublattices μ and ν, including all equivalent sublattices ν translated by lattice vector R, except when $\mu = \nu$ in the first unit cell ($R = 0$).

Rewriting these equations, we have the following eigenvalue problem:

$$(\Theta - TI)E = 0, \qquad \tfrac{3}{2}k_B\Theta_{\mu\nu} = J_{m,0}^{\mu\nu}, \tag{3}$$

where $J_{m,0}^{\mu\nu}$ is the magnetic exchange parameter between sublattices μ and ν, k_B is the Boltzmann constant, I is the identity matrix, $E^{\nu} = \langle e^{\nu}\rangle$, and $\langle e^{\nu}\rangle$ is the average z

component of the unit vector $\langle e_R^{\nu} \rangle$ in the direction of the magnetic moment in sublattice ν. The Curie temperature of the system corresponds to the largest eigenvalue of Θ.[28–31] For disordered systems, a single sublattice may be occupied by more than one atom with different atomic concentrations. In this case, the effective exchange parameters are used in the calculations of the Curie temperature. For example, for a ternary stoichiometric $B2$ structure, the sublattice (0,0,0) is occupied by Ni and Ga atoms each at 50 at. %, while the sublattice (0.5,0.5,0.5) is occupied by Co atoms. Let us denote an equivalent atom at sublattice (0,0,0) as x. The effective exchange parameter between the Co atom and the x "atoms" is given as[32]

$$J_m^{\text{Co-}X} = 0.5 J_m^{\text{Co-Ni}} + 0.5 J_m^{\text{Co-Ga}}, \tag{4}$$

where $J_m^{\text{Co-Ni}}$ is the exchange parameter between Co atoms in the sublattice (0.5,0.5,0.5) and Ni atoms in the sublattice (0,0,0) and $J_m^{\text{Co-Ga}}$ is the exchange parameter between Co atoms in the sublattice (0.5,0.5,0.5) and Ga atoms in the sublattice (0,0,0). To check the accuracy of this method and validate our numerical technique, we calculated the Curie temperature of the Ni_2MnSn alloy. The Curie temperature was found to be 370 K which is in good agreement with the previous published results of 362 K (Ref. 33) and 373 K (Ref. 34).

In this work, a q-state Pott's model is used in place of the Ising model to take into account the discrete magnetic states of Co and Ni atoms. The Hamiltonian describing the energy of the system is given as

$$H = -\sum_{\langle i,j \rangle} J_m^{ij}(2\delta_{S_i S_j} - 1), \quad \delta_{S_i S_j} = \begin{cases} 1 & \text{if} \quad S_i = S_j, \\ 0 & \text{else}, \end{cases} \tag{5}$$

where $\delta_{S_i S_j}$ is the Kronecker symbol, S_i is the spin state of the lattice site i, and J_m^{ij} corresponds to the magnetic exchange parameters involving sites i and j.[35] Magnetic exchange parameters are positive for atoms interacting ferromagnetically—favoring the same spin state on neighboring lattice sites—and negative for atoms interacting antiferromagnetically—favoring opposite spin states on neighboring lattice sites.

We would like to note that a modified version of the Potts model is considered in this work[36] as we replace the term $\delta_{S_i S_j}$ in the original Potts model by $(2\delta_{S_i Sj} - 1)$. In the original Potts model, when a spin at a given site is flipped, the change in the magnetic energy of the system is half of that obtained by flipping a spin in the Heisenberg model—see Ref. 36. Since the exchange parameters calculated using the SPRKKR software are based on the Heisenberg model, the Potts model has been modified to make it equivalent to the Heisenberg model. In the modified Potts model, the change in energy of the system, when a spin is flipped, is the same as obtained in the Heisenberg model. The validity of this modification is evident when comparing—see below–the good agreement in the Curie temperatures calculated within the MFA and through the Monte Carlo simulations.

The Hamiltonian described in Eq. (5) is solved for specific temperatures using a Monte Carlo simulation scheme. In these simulations, the magnetic states are randomly sampled and accepted or rejected based on the Metropolis algorithm.[37,38] The numerical procedure for the Monte Carlo simulation consists of the following steps:

(1) Select the initial configuration in a random manner. Since the Metropolis algorithm satisfies the condition of ergodicity, the system will always reach the equilibrium state regardless of the initial configuration.

(2) Choose a site, randomly select its new spin state, and calculate the change in the energy of the system, ΔH.

(3) Accept or reject the new state based on the Metropolis algorithm. If ΔH is negative, accept the new state and if this is not the case calculate the acceptance probability of the new spin state, $e^{-\Delta H/K_B T}$. Generate a random number between 0 and 1 and if the random number is less than the acceptance probability, the new state is accepted, otherwise it is rejected.

(4) Move to the next site and follow the procedure outlined above. Once all lattice sites are swept, one Monte Carlo step (MCS) is finished.

(5) Continue the above procedure until equilibrium is reached, and after equilibration collect the statistics from a sufficient number of configurations.

At any given temperature, the magnetization (m), magnetic susceptibility (χ_m), and magnetic specific heat (C_{mag}) of the system can be calculated as[38–40]

$$m = \frac{1}{\sum_i^n N_i} \left(\sum_i^n \frac{q_i N_{\text{max}}^i - N_i}{q_i - 1} \right), \tag{6}$$

$$\chi_m = \frac{1}{k_B T^2} [\langle m^2 \rangle - \langle m \rangle^2], \tag{7}$$

$$C_{\text{mag}} = \frac{1}{k_B T^2} [\langle H^2 \rangle - \langle H \rangle^2], \tag{8}$$

where N_i is the total number of atoms of type i, n is the total number of different (magnetic) atom types, two in this case (Co,Ni), q_i is the total number of magnetic states of atom i, N_{max}^i is the maximum number of identical magnetic states for atom i, k_B is Boltzmann's constant, T is the temperature of the system, $\langle m^2 \rangle$ is the average of the squared magnetization, $\langle H \rangle$ is the average energy of the system, and $\langle H^2 \rangle$ is the average squared energy. The magnetic entropy can then be obtained through integration of the magnetic specific heat.

III. EXPERIMENTAL PROCEDURE

Experiments were performed on different compositions in order to study the effect of atomic ordering on the magnetic properties. Since the study focuses on the effect of disorder on the system properties, compositions other than the stoichiometric ones have been considered. The excess or deficiency of atoms of one type or replacement of an atom in its sublattice by others introduces disorder in the system. The experimental results presented here are being used to assess the effect of configurational disorder, i.e., through deviations from stoichiometry, on the magnetic properties of Co-Ni-Ga alloys including their Curie temperatures. These results will also help us set an estimate for the expected inaccuracy of the methods used to predict the Curie temperature of CoNiGa FSMAs.

TABLE I. Measured Curie and stress-free transformation temperatures and both austenite and martensite lattice parameters of experimentally investigated alloys. M_f, martensite finish, M_s, martensite start, A_s, austenite start, A_f, austenite finish temperatures. Experimental uncertainties of the SQUID measurements are within ±1 K. Extrinsic uncertainties due to inhomogeneities in the composition of the sample or sample-to-sample variation are within ±10 K. Tetra, tetragonal crystal structure; Cubic, cubic crystal structure; RT, room temperature; c, lattice parameter of tetra in z direction.

						Lattice parameter (Å)	
Structure	T_C (K)	M_f (K)	M_s (K)	A_s (K)	A_f (K)	Tetra	Cubic
$Co_{50}Ni_{20}Ga_{30}$	390	210	216	222	236		2.86 (at RT)
$Co_{46.5}Ni_{23}Ga_{30.5}$	341	221	305	262	332	3.84 (c : 3.19) (at RT)	2.87 (at 350 K)

Two single β-phase ($B2$ structure) Co-Ni-Ga alloys with nominal compositions of $Co_{50}Ni_{20}Ga_{30}$ and $Co_{46.5}Ni_{23}Ga_{30.5}$ (in at. %) were prepared by vacuum arc melting of 99.9% Co, 99.95% Ni, and 99.999% Ga. Small pieces were cut and homogenized at 1473 K for 4 h in argon followed by water quenching. The stress-free transformation temperatures and the Curie temperature were found using low-field thermal cycling in a Quantum Design superconducting quantum interference device (SQUID) magnetometer at a heating and cooling rate of 5 K/min^{-1}. The crystal structure of the alloys was determined using a Bruker-AXS D8 x-ray diffractometer with Cu $K\alpha$ (0.154 06 nm) radiation.

IV. RESULTS AND DISCUSSIONS

A. Experimental results

Transformation temperatures and Curie temperatures of the experimentally investigated $Co_{46.5}Ni_{23}Ga_{30.5}$ and $Co_{50}Ni_{20}Ga_{30}$ alloys are listed in Table I. In addition to the transition temperatures, the lattice parameters of the constitutive phases are given in the table. Figure 1(a) presents the x-ray diffraction pattern of the $Co_{46.5}Ni_{23}Ga_{30.5}$ sample after heat treatment at 1473 K for 4 h. The $Co_{46.5}Ni_{23}Ga_{30.5}$ sample crystal structures of the phases present are determined to be $L1_0$ for martensite and $B2$ for austenite. The sample is heated above the austenite finish temperature (350 K) to get the x-ray diffraction pattern of the austenite phase which is determined to be $B2$ [Fig. 1(b)]. The lattice parameters of the $Co_{46.5}Ni_{23}Ga_{30.5}$ sample are determined to be $a = 0.384$ nm and $c = 0.319$ nm for martensite and $a = 0.287$ nm for the $B2$ austenite. Figure 1(c) displays the x-ray diffraction pattern of the $Co_{50}Ni_{20}Ga_{30}$ sample after heat treatment at 1473 K for 4 h, showing the $B2$ austenite structure at room temperature. Since this sample transforms to martensite at a very low temperature (216 K) only the $B2$ phase lattice parameter can be determined. The lattice parameter of the $B2$ austenite phase is found to be $a = 0.286$ nm.

B. *Ab initio* calculations

The Heusler ($L2_1$) structure of Co_2NiGa consists of Ga in the (0,0,0) sublattice, Ni in the (1/2,1/2,1/2) sublattice, and Co in the (1/4,1/4,1/4) and (3/4,3/4,3/4) sublattices as shown in Fig. 2(a). $B2$ is a body-centered cubic (bcc) structure, in which it is *assumed* that the (0,0,0) sublattice is randomly occupied by either Ga or Ni atoms and the (1/2,1/2,1/2) sublattice is occupied by (the majority) Co atoms as demonstrated in Fig. 2(b). Here we note that the actual stable configuration in the $B2$-ordered structure may be different from the configuration assumed in this work, and in fact some further disorder involving atomic exchanges between the Co and (Ni,Ga) sublattices is also possible. At

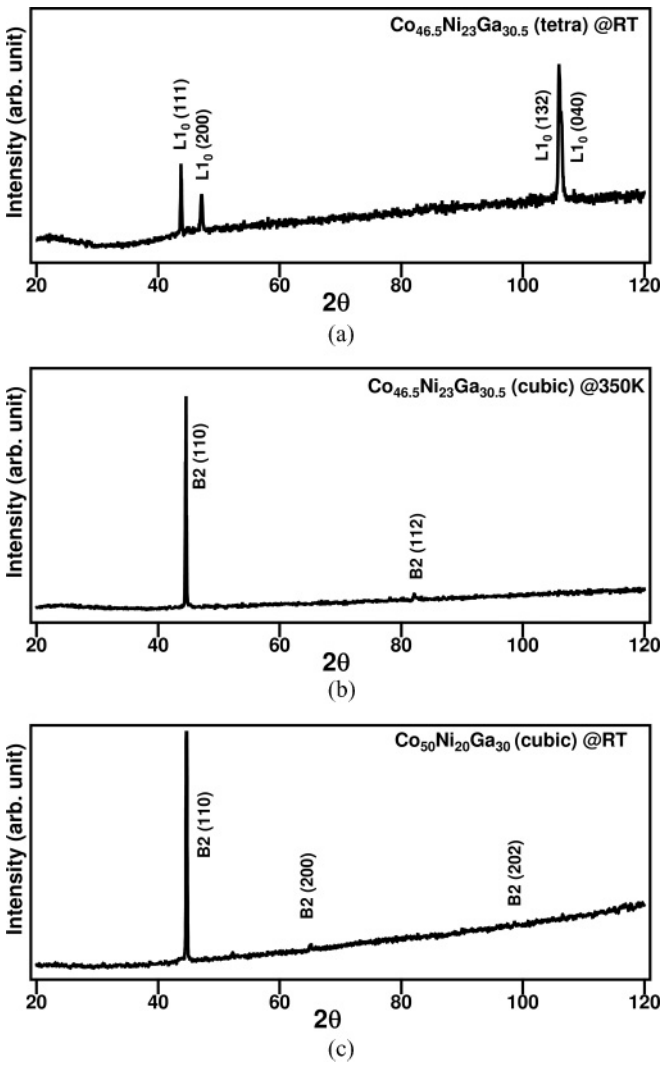

FIG. 1. X-ray diffraction pattern of the (a) tetragonal $Co_{46.5}Ni_{23}Ga_{30.5}$ at room temperature (RT), (b) cubic $Co_{46.5}Ni_{23}Ga_{30.5}$ at 350 K, and (c) cubic $Co_{50}Ni_{20}Ga_{30}$ at RT, indicating the structures of the constitutive phases. $L1_0$, tetragonal martensite; $B2$, cubic austenite.

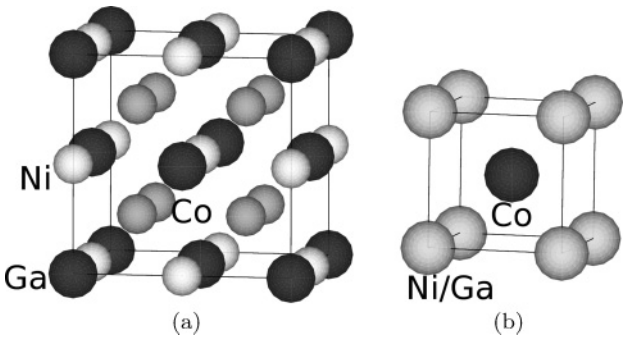

FIG. 2. Structure of (a) ordered ($L2_1$) system with Co, Ni, and Ga atoms occupying their own sublattices, (b) disordered ($B2$) system with the Co atom in sublattice I and Ni and Ga atoms occupying the sublattice II. In *ab initio* calculations (for stoichiometric compositions), the Ni and Ga atom contribution is 50% at each site of sublattice II, while in Monte Carlo simulations, they are randomly distributed on sublattice II of the supercell.

the same time, the simplistic model for $B2$ ordering in this ternary system may not be valid if significant short-range order is still prevalent at elevated temperatures. For the case of the stoichiometric alloys we compare only a fully ordered ($L2_1$) and a partially B2-type-ordered configuration. In the case of the off-stoichiometric alloys, we examined multiple degrees of configurational order by considering $B2$-type configurations as well as $L2_1$-type ordering with different site occupations while the overall composition was retained.

The equilibrium lattice parameters and calculated properties are listed in Table II. We note that the SPRKKR code is unable to correctly predict the fact that the tetragonal structure (i.e., martensite) is more stable than the cubic structure under shear deformations, and we have used results obtained earlier[22,24] and assumed that the martensite has a c/a ratio of approximately $\sim$1.4. The reason for this is unclear but a possible explanation may lie in rather subtle effects related to the effect of symmetry breaking (under the tetragonal distortion) on d electrons of Co and Ni. For all the structures, the equilibrium lattice parameter ($a_{\min}$) corresponding to the lowest energy of the system has been calculated using the SPRKKR code. In previous calculations the tetragonal distortions of $B2$ structures were fully relaxed, while in this work the structure can only relax with constant C/A ratio. As a result, the lattice parameters obtained in these calculations for tetragonal distorted structures are smaller than in previous calculations (as well as experiments). Overall, the lattice parameters and magnetic moments per Co atom

TABLE II. Calculated data for lattice parameters, magnetic moment, and Curie temperature for Co-Ni-Ga alloys. The alloy compositions are stoichiometric unless otherwise stated. $L2_1$ (Tetra) and $B2$ (Tetra) denote the tetragonal distortion of $L2_1$ and $B2$ structures obtained by considering $c/a = 1.4$.

Structure CoNiGa	Order parameter[a]	Lattice parameter at 0 K (Å)	Magnetic moment (μ_B/Co atom)	Curie temperature (K)	
				MFA	MCS
		Alloy composition $x_{Co} = 0.5$, $x_{Ni} = 0.25$, $x_{Ga} = 0.25$			
$L2_1$ (Cubic)	1.0	5.62 (5.68[b])	1.143 (1.262[b], 1.335[c])	423	445
$L2_1$ (Tetra)	1.0	3.56 (3.59[b])	1.281 (1.395[b], 1.46[c])	510	510
$B2$ (Cubic)	0.0	2.81 (2.84[b])	0.898 (1.083[b])	252	275
$B2$ (Tetra)	0.0	2.52 (2.74[b])	1.231 (1.133[b])	413	430
		Alloy composition $x_{Co} = 0.5$, $x_{Ni} = 0.2$, $x_{Ga} = 0.3$			
$B2$ (Cubic)	0.0	2.79	0.7364	169	
$B2$ (Tetra)	0.0	2.51 (2.733[d])	1.0441	262 (432[e],425[d])	
$L2_1$[f] (Cubic)	0.5	5.58	0.77	194	
$L2_1$[f] (Tetra)	0.5	3.546	1.049	277	
$L2_1$[g] (Cubic)	1.0	5.577	0.858	250	
$L2_1$[g] (Tetra)	1.0	3.543	1.065	297	
		Alloy composition $x_{Co} = 0.465$, $x_{Ni} = 0.23$, $x_{Ga} = 0.305$			
$B2$ (Cubic)	0.0	2.80	0.8095	164	
$B2$ (Tetra)	0.0	2.514	1.0543	272 (373[e])	
$L2_1$[h] (Cubic)	0.847	5.58	0.7523	209	
$L2_1$[h] (Tetra)	0.847	3.545	0.98	295	
$L2_1$[i] (Cubic)	1.0	5.607	0.9762	280	
$L2_1$[i] (Tetra)	1.0	3.548	1.0966	355	

[a]Order parameter $(x_{Ni}^{III} - x_{Ni}^{IV})/x_{Ni}$, 1 for fully ordered, 0 for fully disordered.
[b]Arróyave *et al*. (Ref. 22); structure obtained by full relaxation of the tetragonal distortion of $L2_1$ structure.
[c]Siewert *et al*. (Ref. 24).
[d]Oikawa *et al*. (Ref. 10); alloy composition $x_{Co} = 0.45$, $x_{Ni} = 0.25$, $x_{Ga} = 0.3$.
[e]Sarma *et al*. (Ref. 41).
[f]Sublattice occupation: 100% Co on sublattices I and II, 60% Ni and 40% Ga on sublattice III, 20% Ni and 80% Ga on sublattice IV.
[g]Sublattice occupation: 100% Co on sublattices I and II, 80% Ni and 20% Ga on sublattice III, 100% Ga on sublattice IV.
[h]Sublattice occupation: 93% Co and 7% Ni on sublattices I and II, 78% Ni and 22% Ga on sublattice III, 100% Ga on sublattice IV.
[i]Sublattice occupation: 93% Co and 7% Ga on sublattices I and II, 92% Ni and 8% Ga on sublattice III, 100% Ga on sublattice IV.

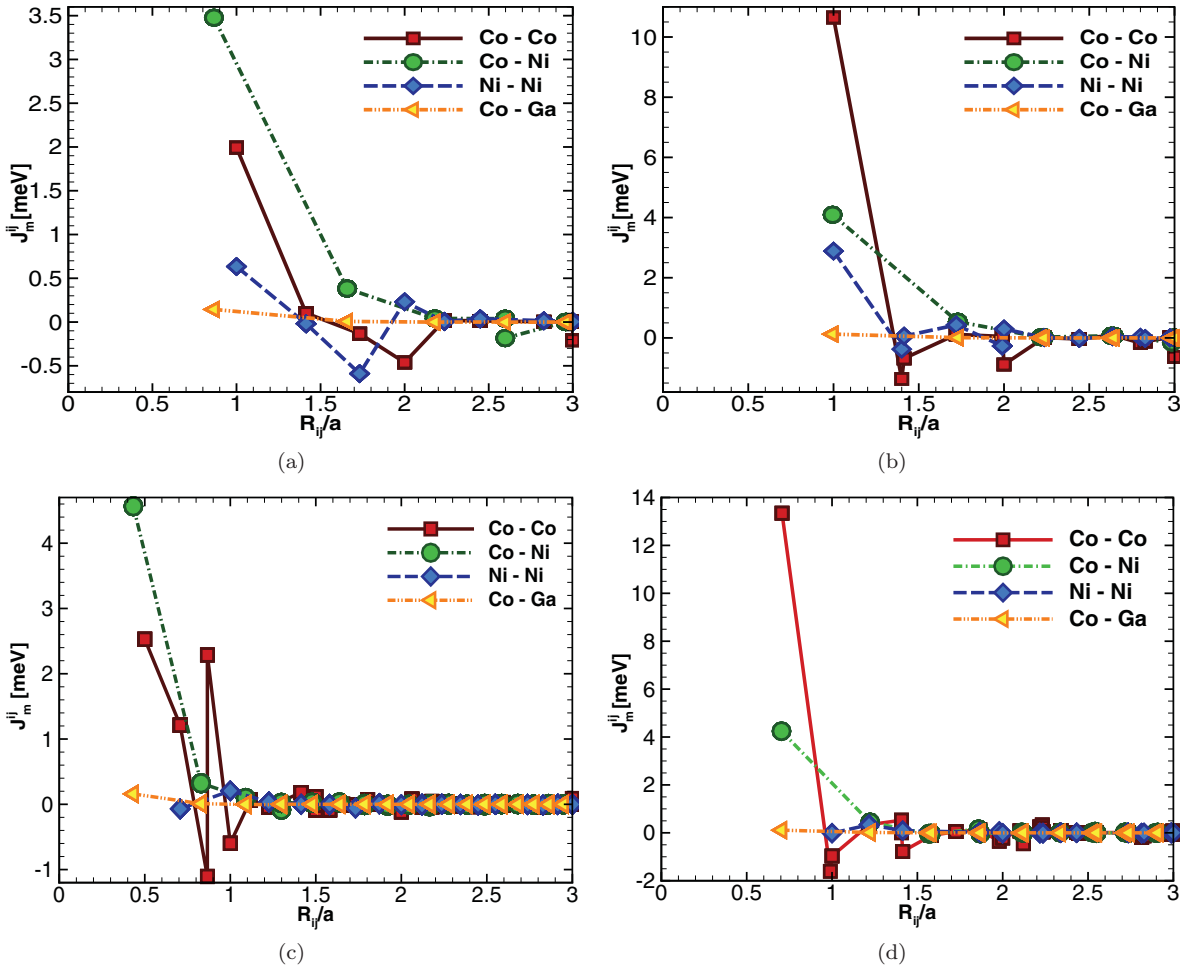

FIG. 3. (Color online) Magnetic exchange interaction parameters J_m^{ij} between an atom i and its neighbor j located at a distance of R_{ij} for (top) disorderedand (bottom) ordered austenite and martensite phases. The distances are normalized with respect to the lattice parameter A. Notice the variation in the values of the vertical scale.

obtained in these calculations are in good agreement with the previous calculations and experimental work. In agreement with previous theoretical studies,[22,24] the SPRKKR results suggest that the total magnetic moment increases upon tetragonal distortion. This observation is in agreement with general trends observed in experimental studies of Co-Ni-Ga alloys.[42] When comparing the total magnetization (normalized per Co atom) of the ordered vs disordered stoichiometric martensite [$L2_1$ (Tetra) and B2 (Tetra), respectively, in Table II], one can see that increased order leads to larger magnetization, which is also in agreement with previous calculations[22] as well as experiments.[9] In fact, Dai *et al.*[9] suggest that for stoichiometric Co_2NiGa martensite, ordering induces a significant (about 30%) increase in the magnetization.

The magnetic exchange parameters calculated for cubic and tetragonal systems of ordered and disordered structures using the equation proposed by Liechtenstein *et al.*[27] are plotted in Fig. 3 (only for stoichiometric compositions) and reported in Table III. In all cases, magnetic exchange interactions between nearest-neighbor Co-Co, Ni-Ni, and Co-Ni atoms are significant (on the order of a few meV). Those between Ga and neighboring atoms are very small as evident from the Co-Ga interaction in Fig. 3. Thus, other magnetic interactions

TABLE III. Magnetic exchange parameters calculated in these simulations. $L2_1$ (Tetra) and $B2$ (Tetra) denote the tetragonal distortions of $L2_1$ and $B2$ structures obtained by considering $c/a = 1.4$.

		Magnetic exchange parameters (J_m^{ij})			
Atoms	Distance (R_{ij}/a)	$L2_1$	$L2_1$ (Tetra)	$B2$	$B2$ (Tetra)
Co-Co	0.5	2.528	13.45		
	0.7		−1.58		
	0.707	1.212	−0.89		
	0.866	0.591	0.335		
	1.0	−0.597	−0.747	1.99	10.648
	1.4				−1.364
	1.414			0.1	−0.683
	2.0			−0.46	−0.883
Co-Ni	0.433	4.566			
	0.497		4.20		
	0.866			3.477	
	0.995				4.093
Ni-Ni	0.707	−0.07	−0.01		
	0.86		0.336		
	1.0	0.206	0.095	0.634	2.88
	1.732			−0.589	0.43

involving Ga have been omitted from the graphs and are not considered in the Monte Carlo simulations. For Co-Co interactions, for a dimensionless distance (R_{ij}/a) of 0.866 in the ordered cubic structure,there are two values of magnetic exchange parameters. The different values are due to the different mediating atoms, as in real-space approaches the final values are not averaged.[29] To clarify this point, consider a pair of Co atoms situated at the (0.25,0.25,0.25) and (0.75,0.75,0.75) positions, respectively. In the $L2_1$ structure, the atom occupying the (0.5,0.5,0.5) position can be Ni or Ga. This atom is identified as the "mediating" atom in this work. The large values of exchange parameters are between Co atom pairs mediated by Ni atoms and the smaller values for Co atom pairs mediated by Ga atoms. The calculations suggest that Ga atoms essentially screen the magnetic interactions between pairs of Co atoms.

In the context of considering energetic interactions in lattice models, it is usually found that in ordered structures long-range and in disordered structures short-range interactions are important.[18] Now, considering the magnetic exchange parameters plotted in Fig. 3, for cubic ordered structures next-nearest-neighbor and second-nearest-neighbor atomic interactions between Co atoms are significant but for the disordered cubic structures only the next-nearest-neighbor interactions are significant, as expected.

The Curie temperatures calculated using the mean-field approximation—Eqs. (1)–(3)and Monte Carlo simulations for the structures are reported in Table II. In general, the Curie temperatures for the cubic structures are lower than for their tetragonal distortions for both $L2_1$ and $B2$ structures. For the stoichiometric compositions, it can be noted that the Monte Carlo simulations and MFA calculations agree within a few kelvin and therefore the systematic study of the effect of ordering on the Curie temperature of experimental compositions has been carried out using the MFA.

For both compositions $Co_{50}Ni_{20}Ga_{30}$ and $Co_{46.5}Ni_{0.23}Ga_{30.5}$, three structures with varying degrees of ordering are considered. In both compositions, the $B2$ structure denotes the fully disordered structures. In the case of $Co_{50}Ni_{20}Ga_{30}$, the most ordered structure is created with the $L2_1$ structure when sublattices I and II are occupied by Co atoms, sublattice III by 80 at. % Ni and 20 at. % Ga, and sublattice IV by Ga atoms, while a partially ordered structure is created with sublattices I and II occupied by Co atoms, sublattice III by 60 at. % Ni and 40 at. % Ga, and sublattice IV by 20 at. % Ni and 80 at. % Ga. For the $Co_{46.5}Ni_{0.23}Ga_{30.5}$ composition, in the highly ordered structure, sublattices I and II are occupied by 93 at. % Co and 7 at. % Ga, sublattice III by 92 at. % Ni and 8 at. % Ga, and sublattice IV by Ga atoms, while for the partially disordered structure, sublattices I and II are occupied by 93 at. % Co and 7 at. % Ni, sublattice III by 78 at. % Ni and 22 at. % Ga, and sublattice IV by Ga atoms.

The results in Table II show that the Curie temperature is lowest for the disordered structures and highest for the ordered structures. The Curie temperature for ordered systems is expected to be higher than that for disordered systems, since in ordered systems, due to long-range ordering, the exchange parameters are expected to be significant up to three or more atomic shells. In the case of disordered systems, usually the exchange parameters are significant only between nearest neighbors. This trend can be seen in the stoichiometric cubic structures in Table III.

We note that the Curie temperature obtained in the experiments is higher than that in the MFA calculations, in some cases differing by about 100 K. In a similar study on NiMnGa FSMAs, Buchelnikov *et al.*[40] observed the same trends and ascribed the discrepancy between experiments and calculations to the neglect of the magnetostructural coupling when dealing with structures undergoing martensitic transitions, as well as to the neglect of nonlocal CPA corrections as the SPRKKR code considers only single-site CPA calculations of the magnetic exchange parameters J_m^{ij}. Table II shows that for a given composition (in the off-stoichiometry configurations) an increase in the configurational order (simulated in this case through changes in the site occupancy of $L2_1$ structures) leads to an increase in the magnitude of the magnetic exchange constants, which in turn results in higher T_c. In fact, the calculations of T_c for the ordered structure for the experimental compositions are close to the values obtained in the experiments. Whether this is because the experimental alloys are in fact not fully disordered cannot be ascertained at the moment, and further analysis of these compositions with varying site occupations and numerical techniques is required.

The densities of states (DOSs) of the stoichiometric systems have been plotted in Fig. 4. The figure shows that, as calculated previously by one of the authors[22] and other groups,[24] the electronic structure is dominated by d-electronic states. As in previous works, the Co and Ni d states seem to hybridize. Moreover, the plot for the ordered cubic structure suggests that the Fermi level is located in an unstable region in which antibonding states are dominant in the case of the minority states. The electronic density of states for the disordered phases shows the usual smearing of the electronic band structure due to disorder. The disordered electronic DOS, however, maintains the general trends observed for the ordered structures. The calculations using plane waves and pseudopotentials published previously[22] suggest that the stabilization of the tetragonal structures is due to the displacement of antibonding states further up in the energy scale. The approximations used in the SPRKKR method are not able to show this.[43]

C. Monte Carlo simulations

For the Monte Carlo simulations, the simulation domain was created by replicating cubic and tetragonal unit cells. The simulation domain consists of 4096 atoms of Co and 2048 atoms each of Ni and Ga. As will be seen below, the size of the simulation domain is sufficient to simulate the magnetic behavior of these systems.[39,40] Also, since the real crystal lattice is used, the number of neighboring atoms will vary depending upon the atom type and the distance between the atoms. As discussed above, the magnetic exchange interactions between Ga and Co or Ni are very small and are therefore neglected in the simulations. From the *ab initio* calculations, the local magnetic moments for Co and Ni are $\sim 1\mu_B$ and $\sim 0.5\mu_B$. Thus, in these simulations it is assumed that Co has three discrete magnetic states while Ni has two discrete magnetic states, estimating the number of magnetic

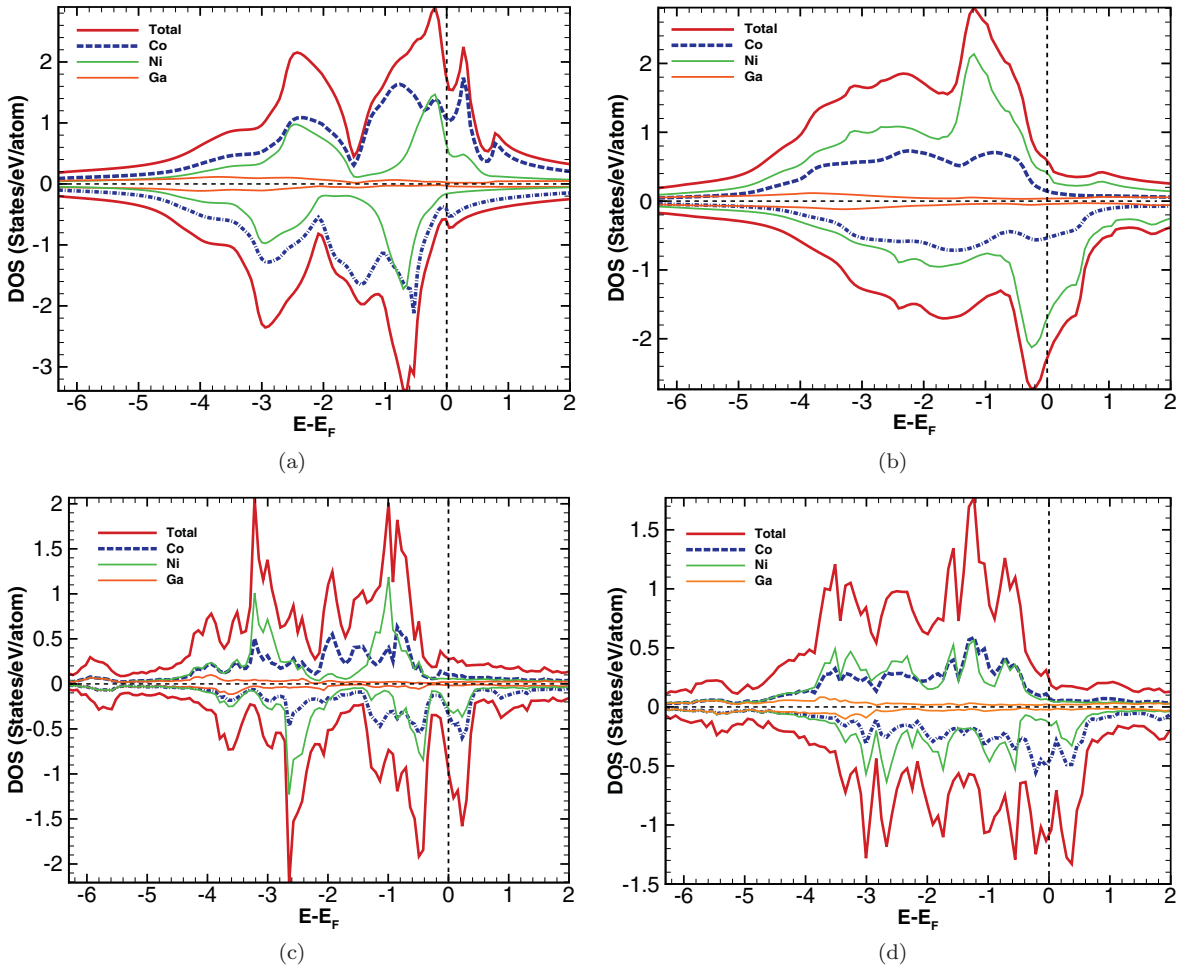

FIG. 4. (Color online) Calculated density of states (DOS) for (a) disordered cubic, (b) disordered tetragonal, (c) ordered cubic, and (d) ordered tetragonal structures. Vertical dotted lines correspond to the Fermi energy level.

states as $2S + 1$. A (3-2)-state Potts model has therefore been used in these calculations. The temperature range explored in these calculations varies from 30 to 600 K. At each discrete temperature step, system equilibration was performed for 50 000 Monte Carlo steps. After equilibration, the energy (H) and magnetization (m) of the system are collected every 100 steps and averaged over 500 configurations. Periodic boundary conditions are used in all the simulations.

The first step in performing the Monte Carlo simulations is to study the effect of the simulation domain size on the properties under consideration. In this regard, the normalized magnetization and specific heat were studied for the $L2_1$ cubic system with supercell size varying from 3 to 9 unit cells (432 to 11 664 atoms in the supercell). The results are plotted in Fig. 5. From the figure it is clear that for systems with 3456 atoms (6 unit cells) the system size is sufficiently large to nullify the effect of the boundary on the system properties. As stated above, in these calculations we have considered a supercell with 8192 atoms (8 unit cells), so our results are well converged.

Figure 6(a) shows the variation of the normalized magnetization with temperature. A zero value of the normalized magnetization means paramagnetic behavior of the system, while a value of 1 is an indication of ferromagnetic behavior. At high temperatures, all the systems behave paramagnetically. As the temperature decreases, the magnetization starts increasing, initiating the magnetic transformation from the paramagnetic to the ferromagnetic state. To ascertain the exact temperature of the magnetic transformation, the magnetic susceptibility is plotted as a function of temperature in Fig. 6(b). The peak in the susceptibility is located at the transition temperature.

The transition temperatures for the disordered systems are significantly lower than the transition temperatures of the ordered systems. The difference is the consequence of the long -range ordering (LRO) in ordered systems and short-range ordering (SRO) in disordered systems. At higher temperatures, the spin states of the atoms are aligned in a random direction. With decrease in temperature, the spin states start aligning in the same direction as their neighbors. As a result, for LRO systems the spin alignment is completed at much higher temperatures as compared to SRO systems.

The above findings are in good agreement with the experimental results obtained by studying the dependence of magnetization on the magnetic field. The higher the Curie temperature, the higher the saturation magnetization of the system. The saturation magnetization of the ordered system in Co_2NiGa alloys (69.3 emu/g) has been found to be

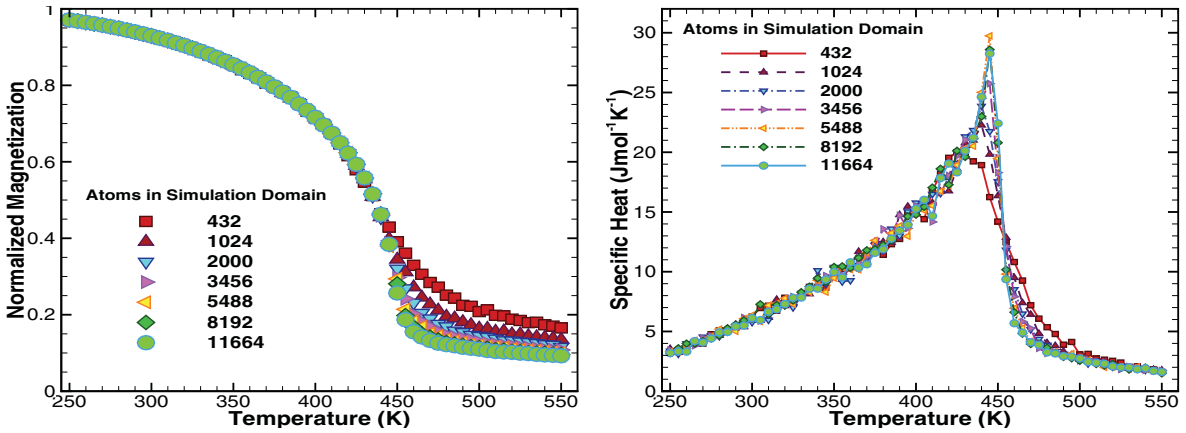

FIG. 5. (Color online) Effect of simulation domain size on the magnetization and specific heat of the system. A supercell with 3456 or more atoms is sufficiently large to nullify the effect of boundary conditions. A supercell with 8192 atoms (equivalent to replicating the $L2_1$ unit cell eight times or the $B2$ unit cell 16 times in all three directions) is considered in this work.

40% greater than in the disordered systems (50.1 emu/g).[9] Moreover, Co-rich alloys have been found to have higher saturation magnetization[12,44] since Co atoms—having higher magnetic moment—tend to introduce more order into the systems. Also, annealing of Co-Ni-Ga alloys results in higher saturation magnetization,[8,12] and this is consistent with an increase in the degree of order of the alloys, even with full ordering into an $L2_1$-type configuration.

The magnetic specific heat of the system calculated using Eq. (8) is plotted in Fig. 6(c). As evident from the figure, the specific heat of the systems increases with decreasing temperature. Near the magnetic transition temperature, the specific heat increases at a very high rate, reaching a peak value at the transition temperature. With further cooling the specific heat decreases at a very fast rate. The magnetic entropy of the systems as a function of temperature is calculated using

$$S_{\mathrm{mag}}(T) = \int_0^T \frac{C_{\mathrm{mag}}}{T} dT. \tag{9}$$

From Fig. 6(a), at low temperatures all the systems have very low entropy. In close vicinity to the magnetic transition temperature, the entropy increases and saturates once the transition temperature is reached. The saturation value of the entropy is consistent with the results for the saturation magnetic entropy obtained using[40]

$$S_{\mathrm{mag,sat}} = R \sum_i \frac{N_i}{N} \ln(2S+1), \tag{10}$$

where i represents a magnetic atom (Co or Ni), N is the total number of magnetic atoms (Co and Ni), S is the spin state of the ith atom, and R is the universal gas constant. The theoretical saturation entropy is calculated to be 8.01 J mol^{-1} K^{-1}. This value is in good agreement with the results of the Monte Carlo simulations shown in Fig. 6(d). The difference between the entropy of ordered and disordered structures is shown in Figs. 6(e) and 6(f). From these figures, for the ordered systems, the difference between the entropy of the cubic structure and that of its tetragonal distortion is small, owing to the small difference in the magnetic transition temperatures. In the case of the disordered structure, the entropy difference is large due to the large difference in the transition temperatures. Thus, in the case of disordered structures, the magnetic entropy has a significant effect on the stability of the structures. This observation is rather important as the relative stability of the cubic and tetragonal structures determines the transformation temperature M_s. The M_s temperature depends on the energy difference between the two crystal structures as well as on the difference in their entropies. For the same energy difference, a higher entropy of the cubic phase results on a lower M_s. Assuming that vibrational contributions to the entropy difference of the cubic and tetragonal structures remain the same regardless of the order state, large differences in the magnetic entropies of the cubic and tetragonal states will play a dominant role in controlling the M_s. The effect of ordering on the magnetic thermodynamic properties of the cubic (austenite) and tetragonal (martensite) structures can therefore explain the effects of aging on the martensitic transformation temperatures observed in many Heusler FSMA systems.

V. CONCLUSION

In this work, we have investigated the effect of atomic ordering on the magnetic properties of Co_2NiGa alloys at stoichiometric and off-stoichiometric compositions. Theoretical calculations and experiments have been performed with different compositions to simulate ordering and disordering effects. The results for the magnetic exchange parameters show that ordered structures possess long-range ordering while disordered structures are short-range ordered. This trend can also be deduced from the Curie temperatures calculations using the MFA, with ordered structures having higher Curie temperatures than disordered structures. The results for the Curie temperatures of experimental compositions agree with numerical calculations for ordered structures. These results suggest atomic ordering in the alloys during annealing; further work is required on the effect of heat treatment on the atomic ordering and site occupations.

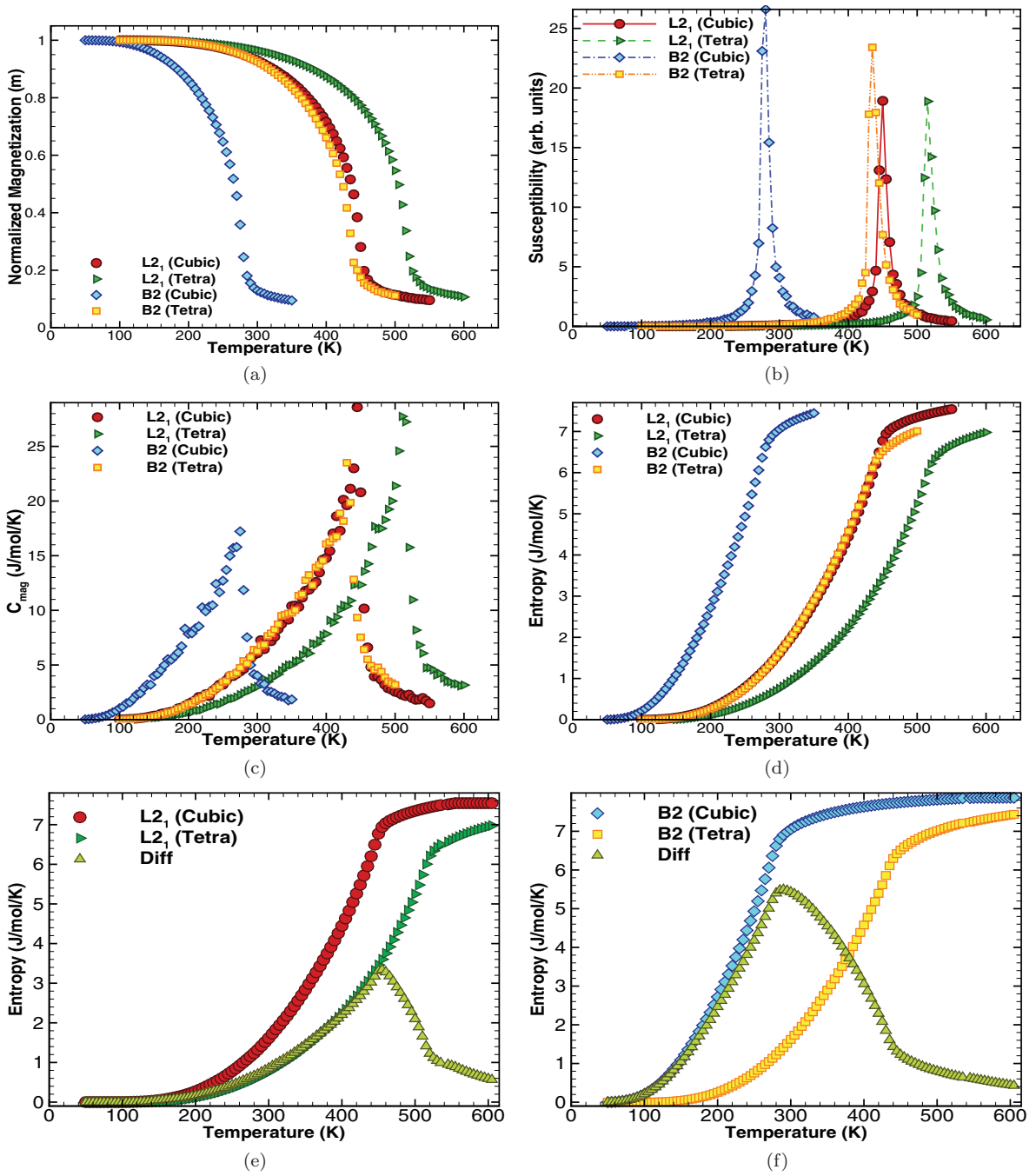

FIG. 6. (Color online) Results of the Monte Carlo simulations for ordered and disordered systems: (a) magnetization, (b) magnetic susceptibility, (c) magnetic specific heat, (d) magnetic entropy, and (e),(f) entropy difference between (e) the ordered ($L2_1$) cubic structure and its tetragonal distortion and (f) the disordered ($B2$) cubic structure and its tetragonal distortion.

Further analysis of the magnetic properties (including Curie temperature, magnetic susceptibility, specific heat, and entropy) of stoichiometric Co_2NiGa alloys with $L2_1$- and B2-type ordering has been carried out using Monte Carlo simulations. These results suggest that ordering seems to screen ferromagnetic interactions when the alloys have $B2$-type ordering. This screening is accompanied by a decrease in the saturation magnetization as well as the Curie temperature of the alloys, in accordance with empirical evidence obtained from investigations on Co-Ni-Ga as well as other FSMAs. $B2$-type ordering results in a higher magnetic entropy contribution for the martensitic transformation than $L2_1$ ordering in Co_2NiGa. Future investigations on the quantitative effect of the magnetic entropy on the martensitic transformation characteristics can provide important insights into the structural transformation and stability in these alloys.

ACKNOWLEDGMENTS

The authors would like to acknowledge the National Science Foundation (Grant Nos. DMR-0844082 and

DMR-0805293) for support to complete this work. First-principles calculations were carried out in the Chemical Engineering cluster of Texas A& M University, the Texas A&M Supercomputing Facility, and the Ranger cluster at the Texas Advanced Computing Center (TACC) at the University of Texas in Austin.

[1] V. A. Chernenko, E. Cesari, V. V. Kokorin, and I. N. Vitenko, Scr. Mater. **33**, 1239 (1995).
[2] S. J. Murray, M. Marioni, S. M. Allen, R. C. O'Handley, and T. A. Lograsso, Appl. Phys. Lett. **77**, 886 (2000).
[3] K. Ullakko, J. K. Huang, C. Kantner, R. C. O'Handley, and V. V. Kokorin, Appl. Phys. Lett. **69**, 1966 (1996).
[4] J. Pons, E. Cesari, C. Segui, F. Masdeu, and R. Santamarta, Mater. Sci. Eng. A **481**, 57 (2008).
[5] H. E. Karaca, I. Karaman, B. Basaran, Y. Ren, Y. I. Chumlyakov, and H. J. Maier, Adv. Funct. Mater. **19**, 983 (2009).
[6] M. Acet, E. Duman, E. F. Wassermann, L. Manosa, and A. Planes, J. Appl. Phys. **92**, 3867 (2002).
[7] S. Ghosh and B. Sanyal, J. Phys.: Condens. Matter **22**, 346001 (2010).
[8] M. Wuttig, J. Li, and C. Craciunescu, Scr. Mater. **44**, 2393 (2001).
[9] Xuefang Dai, Guodong Liu, Yangxian Li, Jingping Qu, Jia Li, Jinglan Chen, and Guangheng Wu, J. Appl. Phys. **101**, 09N503 (2007).
[10] K. Oikawa, T. Ota, F. Gejima, T. Ohmori, R. Kainuma, and K. Ishida, Mater. Trans.-JIM **42**, 2472 (2001).
[11] Jian Liu, Mingxu Xia, Yanlu Huang, Hongxing Zheng, and Jianguo Li, J. Alloys Compd. **417**, 96 (2006).
[12] B. Kostrubiec, K. Prusik, Ł. Madej, and H. Morawiec, Solid State Phenomena **130**, 141 (2007).
[13] E. Dogan, I. Karaman, Y. I. Chumlyakov, and Z. P. Luo, Acta Mater. **59**, 1168 (2011).
[14] A. Planes, E. Vives, and T. Castán, Phys. Rev. B **44**, 6715 (1991).
[15] A. Planes, L. Manosa, E. Vives, J. Rodriguez-Carvajal, M. Morin, G. Guenin, and J. L. Macqueron, J. Phys.: Condens. Matter **4**, 553 (1992).
[16] E. Obradó, C. Frontera, L. Mañosa, and A. Planes, Phys. Rev. B **58**, 14245 (1998).
[17] F. Lanzini, R. Romero, and M. L. Castro, Intermetallics **16**, 1090 (2008).
[18] F. Lanzini, R. Romero, M. Stipcich, and M. L. Castro, Phys. Rev. B **77**, 134207 (2008).
[19] W. Ito, M. Nagasako, R. Y. Umetsu, R. Kainuma, T. Kanomata, and K. Ishida, Appl. Phys. Lett. **93**, 232503 (2008).
[20] R. Kainuma, F. Gejima, Y. Sutou, I. Ohnuma, and K. Ishida, Mater. Trans.-JIM **41**, 943 (2000).
[21] S. N. Kaul, B. Annie D' Santhoshini, A. C. Abhyankar, L. Fernández Barquín, and P. Henry, Appl. Phys. Lett. **89**, 093119 (2006).
[22] R. Arróyave, A. Junkaew, A. Chivukula, S. Bajaj, C. Y. Yao, and A. Garay, Acta Mater. **58** 5220 (2010).
[23] A. Ayuela, J. Enkovaara, and R. M. Nieminen, J. Phys.: Condens. Matter **14**, 5325 (2002).
[24] M. Siewert, M. E. Gruner, A. Dannenberg, A. Hucht, S. M. Shapiro, G. Xu, D. L. Schlagel, T. A. Lograsso, and P. Entel, Phys. Rev. B **82**, 064420 (2010).
[25] H. Ebert, The Munich SPR-KKR package, version 5.4, (2010).
[26] H. Ebert, Electron. Struct. Phys. Properties Solids **535**, 191 (2000).
[27] A. I. Liechtenstein, M. I. Katsnelson, and V. A. Gubanov, J. Phys. F **14**, L125 (1984).
[28] E. Şaşıoğlu, L. M. Sandratskii, and P. Bruno, Phys. Rev. B **70**, 024427 (2004).
[29] M. Meinert, J. M. Schmalhorst, and G. Reiss, J. Phys.: Condens. Matter **23**, 036001 (2011).
[30] E. Şaşıoğlu, L. M. Sandratskii, P. Bruno, and I. Galanakis, Phys. Rev. B **72**, 184415 (2005).
[31] P. W. Anderson, Solid State Phys. **14**, 99 (1963).
[32] A. I. Liechtenstein, M. I. Katsnelson, V. P. Antropov, and V. A. Gubanov, J. Magn. Magn. Mater. **67**, 65 (1987).
[33] E. Şaşıoğlu, L. M. Sandratskii, and P. Bruno, Phys. Rev. B **71**, 214412 (2005).
[34] Y. Kurtulus, R. Dronskowski, G. D. Samolyuk, and V. P. Antropov, Phys. Rev. B **71**, 014425 (2005).
[35] Note the change of notation in the exchange parameter J_m^{ij} in equation (5) as compared to $J_{m,0}^{\mu\nu}$ in equations (1)-(3). In equation (5), the magnetic interactions J_m^{ij} are considered between any pair of sites i and j, while $J_{m,0}^{\mu\nu}$ corresponds to an effective magnetic exchange parameter between sublattices μ and ν of an ordered structure, including the sublattices of neighboring unit cells..
[36] P. Meyer, Master's thesis, School of Mathematics and Computing, University of Derby, 2000.
[37] M. E. J. Newman and G. T. Barkema, *Monte Carlo Methods in Statistical Physics* (Oxford University Press, USA, 1999).
[38] T. Castán, E. Vives, P. A. Lindgård, Phys. Rev. B **60**, 7071 (1999).
[39] V. D. Buchelnikov, P. Entel, S. V. Taskaev, V. V. Sokolovskiy, A. Hucht, M. Ogura, H. Akai, M. E. Gruner, and S. K. Nayak, Phys. Rev. B **78**, 184427 (2008).
[40] V. D. Buchelnikov, V. V. Sokolovskiy, H. C. Herper, H. Ebert, M. E. Gruner, S. V. Taskaev, V. V. Khovaylo, A. Hucht, A. Dannenberg, M. Ogura *et al.*, Phys. Rev. B **81**, 094411 (2010).
[41] S. Sarma and A. Srinivasan, Adv. Mater. Res. **52**, 103 (2008).
[42] P. J. Brown, K. Ishida, R. Kainuma, T. Kanomata, K. U. Neumann, K. Oikawa, B. Ouladdiaf, and K. R. A. Ziebeck, J. Phys.: Condens. Matter **17**, 1301 (2005).
[43] P. Entel, V. D. Buchelnikov, V. V. Khovailo, A. T. Zayak, W. A. Adeagbo, M. E. Gruner, H. C. Herper, and E. F. Wassermann, J. Phys. D: Appl. Phys. **39**, 865 (2006).
[44] J. Liu, H. X. Zheng, M. X. Xia, Y. L. Huang, and J. G. Li, Scr. Mater. **52**, 935 (2005).